JETIR.ORG ISSN: 2349-5162 | ESTD Year : 2014 | Monthly Issue
JOURNAL OF EMERGING TECHNOLOGIES AND INNOVATIVE RESEARCH (JETIR)
An International Scholarly Open Access, Peer-reviewed, Refereed Journal

DEVELOPMENT OF HIGH COLOUR PURITY RED LIGHT EMITTING Sm DOPED $Gd_2Zr_2O_7$ PHOSPHORS

Neha Sharma[1], Piyush Jha[1], Vinita Garg[2]

[1]Department of Physics, Faculty of Science, Shri Rawatpura Sarkar University, Raipur, Chhattisgarh, 492015, India
[2]Department of Chemistry, D.N. (P.G.) College Gulaothi, Bulandshahr

Abstract : $Gd_2Zr_2O_7:Sm^{3+}$ phosphors with varying samarium concentrations (8–24 mol%) were successfully synthesized using a conventional solid-state reaction method. X-ray diffraction (XRD) confirmed the formation of a single-phase cubic pyrochlore structure, irrespective of Sm^{3+} doping levels, indicating successful incorporation of dopant ions into the host lattice. Photoluminescence (PL) studies revealed characteristic excitation peaks at 275 nm and 409 nm, and emission peaks at 614 nm and 624 nm, corresponding to Sm^{3+} electronic transitions. The optimal PL intensity was achieved at 12 mol% Sm^{3+}, beyond which concentration quenching occurred, attributed to dipole-dipole interactions as supported by Dexter's theory. FTIR analysis further validated the material's phase purity. Thermoluminescence (TL) studies on the 12 mol% sample exhibited glow peaks at 116 °C and 240 °C. The chromaticity coordinates (x = 0.6720, y = 0.3276) confirmed a high color purity (~99.9%) in the red emission region, indicating the phosphor's strong potential for red-emitting optoelectronic applications.

Keywords: $Gd_2Zr_2O_7$:Sm, FTIR, photoluminescence, thermoluminescence.

I. INTRODUCTION

White light-emitting diodes (WLEDs) have gained prominence as a leading lighting technology, favored for their high energy efficiency, extended operational life, environmental compatibility, and compact form factor. A key aspect of enhancing WLED performance lies in the development of advanced phosphor materials capable of efficiently converting excitation energy into visible light while maintaining high color rendering and thermal durability [1]. Among the various types of phosphors, red-emitting ones are especially important, as they significantly influence the color rendering index (CRI) and correlated color temperature (CCT). However, achieving red phosphors with both high quantum efficiency and robust thermal stability continues to be a challenge [2]. Samarium (Sm^{3+})-doped phosphors have emerged as promising candidates due to their characteristic orange-red emission, originating from internal 4f–4f electronic transitions, particularly $^4G_{5/2} \rightarrow {}^6H_J$ (J = 5/2, 7/2, 9/2). Current research focuses on embedding Sm^{3+} ions into various host matrices—such as oxides, vanadates, and pyrochlore structures—to enhance their luminescent output [3]. Among these, $Gd_2Zr_2O_7$, with its stable pyrochlore framework, stands out owing to its excellent chemical durability, low phonon energy, and high suitability for rare-earth ion substitution. Sm^{3+}-doped $Gd_2Zr_2O_7$ phosphors, in particular, exhibit strong red emission when excited by near-ultraviolet (UV) light, making them suitable for integration into near-UV pumped WLED systems. Moreover, the presence of Gd^{3+} ions can facilitate energy transfer mechanisms that may further enhance Sm^{3+} luminescence [4]. The emission characteristics of these materials can be fine-tuned by adjusting dopant concentrations and synthesis conditions, allowing for performance optimization in real-world lighting applications. These phosphors offer advantages such as low thermal quenching, structural resilience, and stable chromaticity under high-power operation. Consequently, Sm^{3+}-activated $Gd_2Zr_2O_7$ materials are being investigated as effective solutions to address the red emission gap in conventional YAG:Ce^{3+}-based WLEDs [5]. Their inclusion can improve CRI and produce more visually comfortable white light. Furthermore, their robustness under thermal and optical stress makes them ideal for demanding environments, including outdoor and industrial lighting [6]. This study aims to synthesize and characterize Sm^{3+}-doped $Gd_2Zr_2O_7$ phosphors and evaluate their photoluminescence (PL) and thermoluminescence (TL) properties. By optimizing the material design, this work contributes to the ongoing advancement of rare-earth-doped red phosphors for next-generation solid-state lighting applications.

II. EXPERIMENTAL

$Gd_2Zr_2O_7$:Sm phosphors with varying Sm concentrations (ranging from 8 mol% to 24 mol%) were synthesized via the solid-state reaction method. The starting materials—Gd_2O_3, ZrO_2, and Sm_2O_3—were weighed according to their stoichiometric ratios and thoroughly mixed using a mortar and pestle. The resulting mixture was transferred to an alumina crucible and calcined in a furnace at 1000 °C for 5 hours. After initial calcination, the samples were ground for 30 minutes and then sintered at 1350 °C for an additional 5 hours. Finally, the sintered $Gd_2Zr_2O_7:Sm^{3+}$ phosphors were manually ground again using an agate mortar for approximately 35 minutes.

III. RESULTS AND DISCUSSION

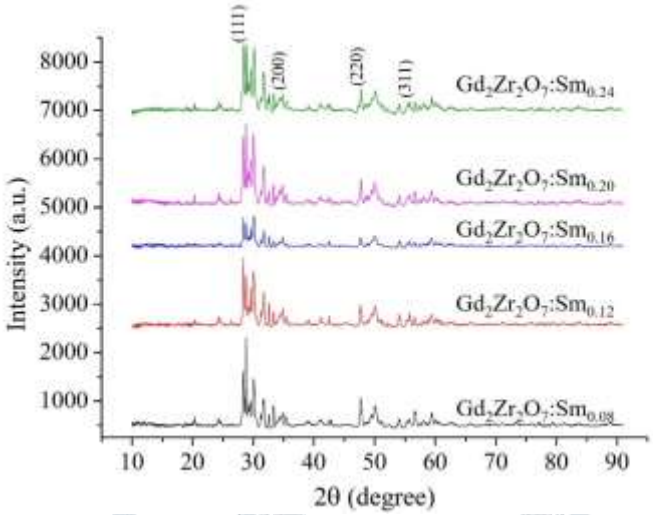

Fig.1 XRD pattern of $Gd_2Zr_2O_7$:Sm (8 to 24 mol%).

Fig.1 presents the X-ray diffraction (XRD) patterns of $Gd_2Zr_2O_7:Sm^{3+}$ phosphors synthesized with varying samarium (Sm^{3+}) concentrations ranging from 8 to 24 mol%. The diffraction peaks observed in all samples are in good agreement with the standard data from the ICSD database (reference code: 98-016-5810), thereby confirming the formation of a single-phase cubic pyrochlore structure with a space group of Fm-3m. This indicates that the incorporation of Sm^{3+} ions into the $Gd_2Zr_2O_7$ host lattice does not significantly alter the crystal structure.

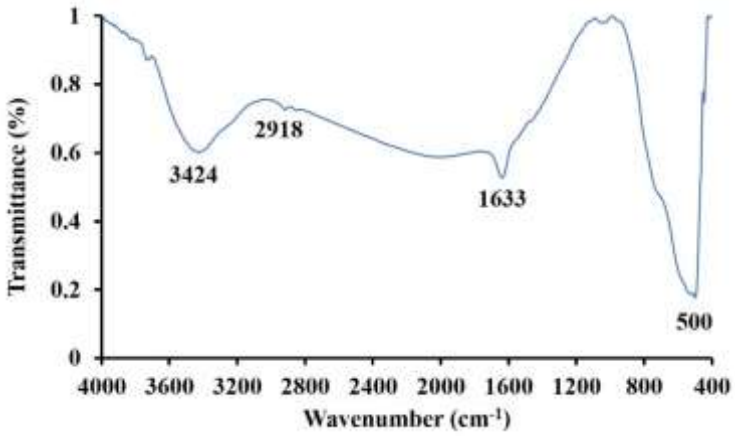

Fig.2 FTIR of $Gd_2Zr_2O_7:Sm_{0.12}$ phosphor.

FTIR (Fourier Transform Infrared Spectroscopy) is a powerful analytical method used to identify a wide range of materials, including organic compounds, polymers, and some inorganic substances. It works by measuring how a sample absorbs infrared light, generating a spectrum that serves as a unique "fingerprint" of the material. FTIR helps detect specific functional groups—such as –OH, –CH, –C=O, and –NH_2—by analyzing the distinct vibrational frequencies of the chemical bonds. Each type of bond within a molecule absorbs infrared light at a characteristic wavelength, allowing for precise identification. 500 cm^{-1} is assigned to Gd-O [7], 1633 cm^{-1} is correspond to C=C [8], 2918 cm^{-1} assigned to C-H [9], 3418 cm^{-1} correspond to O-H [8].

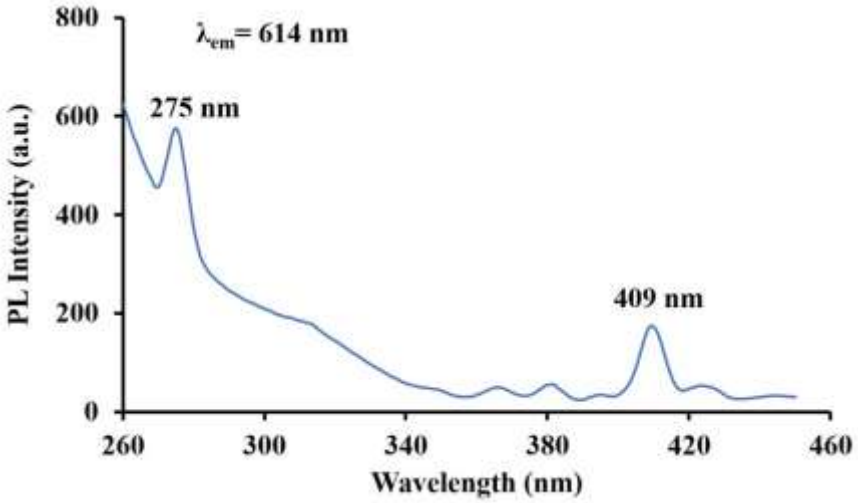

Fig.3 PL Excitation spectra of $Gd_2Zr_2O_7$:Sm phosphor.

The PL excitation spectrum shows two peaks, one highest intensity at 275 nm and lowest intensity 409 nm as shown in Fig.3. Their corresponding transitions are $^6H_{5/2} \rightarrow {}^4F_{5/2}$ and $^6H_{5/2} \rightarrow {}^6P_{3/2}$ transitions. The PL emission spectrum as shown in Fig. 4 depicts two peaks around 614 nm and 624 nm corresponding transition is $^4G_{5/2} \rightarrow {}^6H_{7/2}$ (red-orange visible spectrum) [5]. Fig.5 shows the variation of peak PL intensities with Sm concentration. It is found from figure that for 12 mol% doping concentration the peak PL intensity is highest. After that is decreases with increasing doping concentration of Sm.

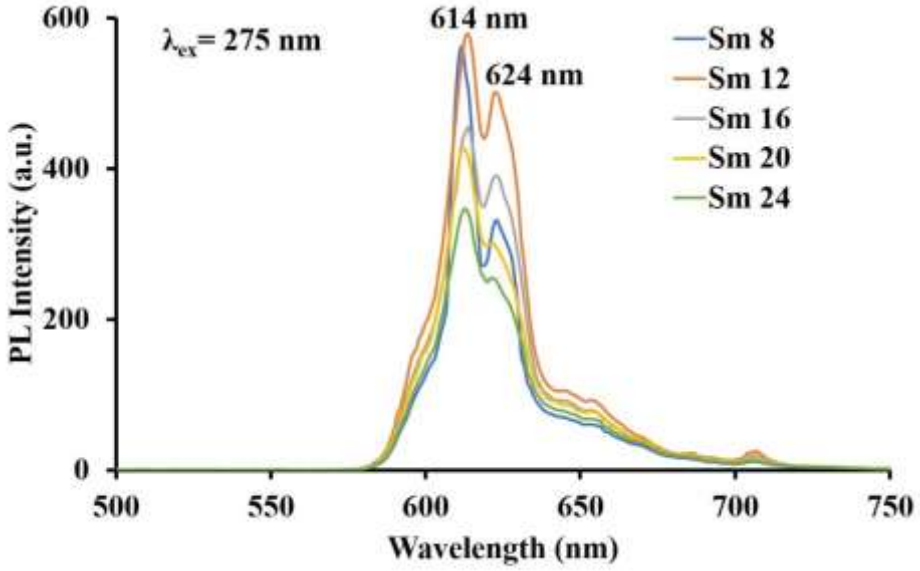

Fig.4 PL emission spectra of $Gd_2Zr_2O_7$:Sm (8 to 24 mol%) phosphor.

Through the Dexter's graph as shown in Fig.6, the slope is found at -1.48. The Q value is found to be 4.44. This is very close to 6 that shows the to the dipole-dipole interaction of Sm ions [10]. The CIE chromaticity diagram generated from photoluminescence (PL) data shows the color emitted by a material when exposed to light. The plotted chromaticity coordinates represent how the emitted color is perceived by the human eye. This diagram helps analyze key properties such as color purity and peak emission wavelength. It is widely used to assess the performance of luminescent materials in devices like LEDs and display panels. Overall, the CIE diagram offers a standardized method for comparing the optical emission characteristics of different materials. Fig.7 depicts the CIE diagram of $Gd_2Zr_2O_7$:$Sm_{0.12}$ phosphor. It is found that the x (0.6720) and y (0.3276) coordinates lie in the red region. The colour purity is found ≈ 99.9%

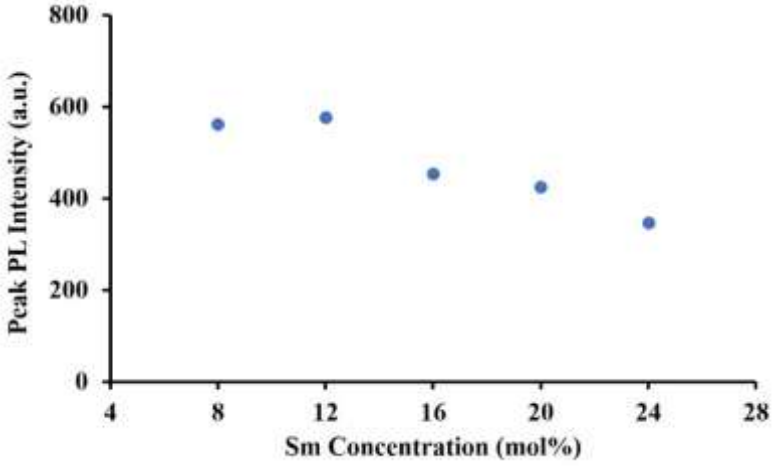

Fig.5 PL intensity variation with Sm concentration.

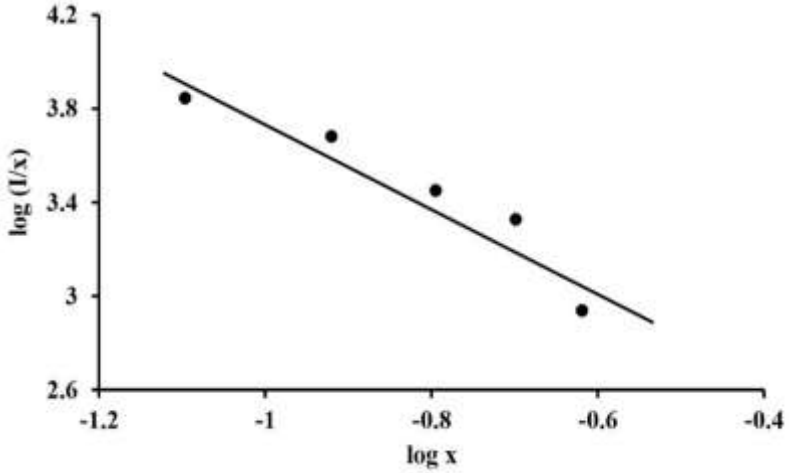

Fig. 6 Plot of log(I/x) versus logx.

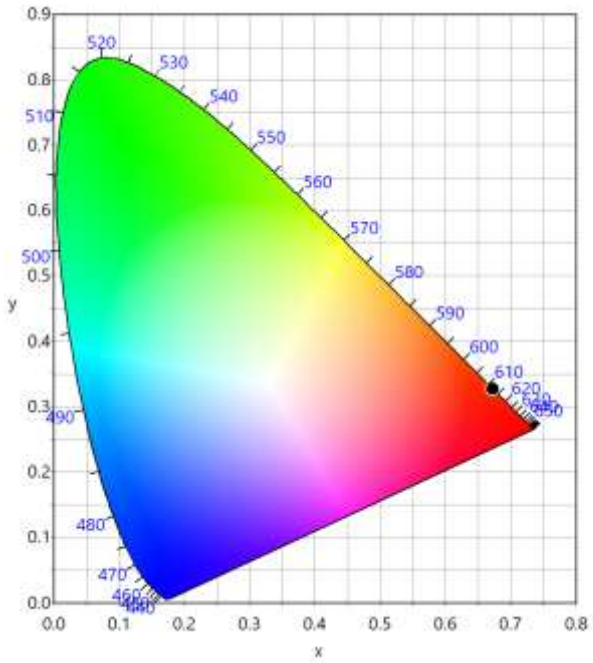

Fig. 7 CIE diagram of $Gd_2Zr_2O_7:Sm_{0.12}$ phosphor.

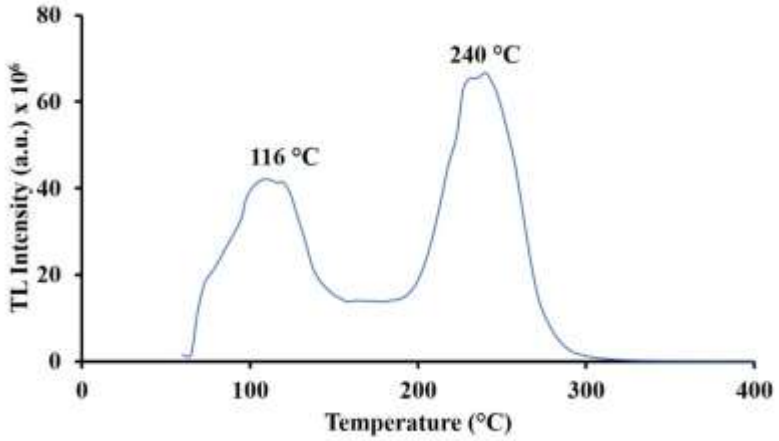

Fig. 8 Thermoluminescence glow curve of $Gd_2Zr_2O_7:Sm_{0.12}$ phosphor.

Thermoluminescence refers to the emission of light from specific materials when they are heated, following earlier exposure to radiation. In radiation dosimetry, it is used to assess the total radiation absorbed by materials such as lithium fluoride by measuring the light released during heating. For dating purposes, it reveals when minerals like quartz or feldspar were last heated, based on the radiation accumulated since that time. This method is commonly used in archaeology to date pottery and in geology to study soil and sediment layers. Fig.8 shows the thermoluminescence glow curve of $Gd_2Zr_2O_7:Sm_{0.12}$ phosphor. Two peaks are found at 116 °C and 240 °C.

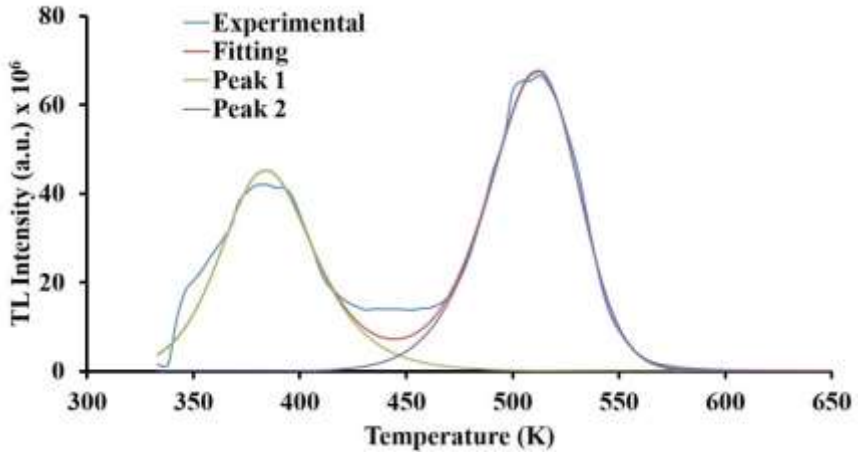

Fig.9 Deconvolution of TL glow curve of $Gd_2Zr_2O_7:Sm_{0.12}$ phosphor (5 min UV exposure).

Fig.9 depicts the Deconvolution of TL glow curve of $Gd_2Zr_2O_7:Sm_{0.12}$ phosphor at 5 min UV exposure. The trapping parameters are calculated by the Chen's methods [11].

Table 1: The values of activation energies and frequency factors calculated by Chen's peak shape method [1].

Sample Name	Peak Number	T_1 (K)	T_m (K)	T_2 (K)	Geometrical factor (μ)	Order of kinetics (b)	Activation energy (eV)	Frequency factor (1/s)
$Gd_2Zr_2O_7:Sm_{0.12}$	Peak 1	360	384	411	0.53	2	0.81	$7.19x10^{11}$
	Peak 2	484.5	512	535	0.45	2	1.49	$7.37x10^{15}$

IV. CONCLUSIONS

This study demonstrated the successful synthesis of $Gd_2Zr_2O_7:Sm^{3+}$ phosphors with a stable cubic pyrochlore structure across all doping levels. Photoluminescence results showed that a Sm^{3+} concentration of 12 mol% yielded the highest emission intensity due to minimized non-radiative losses. The observed concentration quenching beyond this point was consistent with dipole-dipole interactions as indicated by Dexter's analysis. Thermoluminescence studies revealed stable trapping sites with moderate activation energies, making the phosphor suitable for dosimetric applications. Furthermore, the CIE chromaticity analysis confirmed strong red emission with high color purity. These findings suggest that $Gd_2Zr_2O_7:Sm^{3+}$, particularly at 12 mol% Sm^{3+} doping, is a promising candidate for red-emitting devices in display and lighting technologies.

REFERENCES

[1] Chen, J., Xiang, H., Wang, J., Wang, R., Li, Y., Shan, Q., Xu, X., Dong, Y., Wei, C. and Zeng, H., 2021. Perovskite white light emitting diodes: progress, challenges, and opportunities. ACS nano, 15(11): 17150-17174.

[2] Wang, A., Dai, J., Wang, H., Mou, Y., Zhang, Y., Liu, J., Zheng, Z., Peng, Y. and Chen, C., 2019. White light-emitting diodes with ultrahigh color rendering index by red/green phosphor layer configuration structure. IEEE Transactions on Electron Devices, 66(12): 5209-5214.

[3] Hua, Y., Yu, J.S. and Li, L., 2023. Rare-earth and transition metal ion single-/co-doped double-perovskite tantalate phosphors: Validation of suitability for versatile applications. Journal of Advanced Ceramics, 12(5): 954–971.

[4] Gupta, S.K. and Natarajan, V., 2015. Synthesis, characterization and photoluminescence spectroscopy of lanthanide ion doped oxide materials. BARC Newsl, 46:14-21.

[5] Zeng, J., Zhang, K., Teng, Y. and Luo, B., 2025. Influence of non-stoichiometric design concepts on the optical properties of Sm-doped Gd2Zr2O7 transparent ceramics. Ceramics International, 51(12): 16500-16508.

[6] Grzesiak, W., Guzdek, P., Maćków, P., Zaraska, K., Zbieć, M., Jakubowski, M., Obrębski, D., Boguszewicz, P., Solnica, D., Iwanicki, P. and Linke, S., 2018. Smart LED high CRI lighting systems. Microelectronics International, 35(3):181-187.

[7] Munawar, T., Nadeem, M.S., Mukhtar, F., Hasan, M., Mahmood, K., Arshad, M.I., Hussain, A., Ali, A., Saif, M.S. and Iqbal, F., 2021. Rare earth metal co-doped Zn0· 9La0. 05M0. 05O (M= Yb, Sm, Nd) nanocrystals; energy gap tailoring, structural, photocatalytic and antibacterial studies. Materials Science in Semiconductor Processing, 122:105485.

[8] Muñoz-Ruíz, A., Escobar-García, D.M., Quintana, M., Pozos-Guillén, A. and Flores, H., 2019. Synthesis and characterization of a new collagen-alginate aerogel for tissue engineering. Journal of Nanomaterials, 2019(1): 2875375.

[9] He, F., Zhou, L., Fang, M., Sui, C., Li, W., Yang, L., Li, M. and He, X., 2019. Fabrication and simulation analysis of flexible polymethylsilsesquioxane (PMSQ) aerogels by using dimethyl sulfoxide (DMSO) as solvent. Materials & Design, 173:107777.

[10] Van Uitert, L.G., 1967. Characterization of energy transfer interactions between rare earth ions. Journal of the electrochemical society, 114(10): 1048.

[11] Pagonis, V., Kitis, G. and Furetta, C., 2006. *Numerical and practical exercises in thermoluminescence*. New York, NY: Springer New York.